A HYBRID TOPOLOGY OPTIMIZATION APPROACH TO FORCE VISUALIZATION IN REINFORCED CONCRETE STRUCTURES

Kênia A. T. F. Gouveia
keniatogoe@ufmt.br
Institute of Exact and Earth Sciences, Campus Araguaia, Federal University of Mato Grosso
Av. Senador Valdon Varjão, nº 6.390. Barra do Garças, Mato Grosso, Brazil. 78600-00.
Daniel L. Araújo
Sylvia R. M. Almeida
dlaraujo@ufg.br
sylviaalm@gmail.com
School of Civil and Environmental Engineering, Federal University of Goiás
Av. Universitária, 1488, Qd 86, Lt Area. St. Universitário, Goiânia, Goiás, Brazil. 74605-220

Abstract. The Strut-and-Tie Method is a rational approach used to circumvent complexities in the analysis and design of reinforced concrete structures, especially those that do not meet the Bernoulli's hypothesis. This work applies topology optimization techniques to automatically obtain power paths in reinforced concrete structures to be applied in strut-and-tie models. A hybrid formulation of the minimum compliance problem is adopted in which the concrete struts are represented by continuous elements associated with material density and steel reinforcing bars. Bilinear isotropic elastic models are applied to both materials to separate compressive and tensile load paths. In order to eliminate resultant thin bars and provide a force layout applicable in the design practice, a maximum filter is applied at the end of the optimization process. Tikhonov regularization is applied to the potential energy of the structure to solve singular equilibrium equations and check the equilibrium of the extracted solutions in the filtering procedure. Numerical examples are provided to demonstrate the applicability of the proposed formulation.

Keywords: Topology optimization; Hybrid formulation; Strut-and-tie model; Reinforced concrete.

1 Introduction

Reinforced concrete structures with geometric or static discontinuity, such as consoles, openings in beams, deep beams and others that does not meet the Bernoulli's hypotheses, are commonly designed using Strut-and-Tie Models (STM). These models are mainly based on the design of suitable power paths to transfer external forces to the support constraints, for which the connecting strut are idealizations of the compression stress fields linking the tensile fields represented by the tie rods.

Proposals concerning the use of topology optimization techniques for automatic STM generation have emerged in the last 10 years. Bruggi [1] applied a topology optimization approach based on the material distribution and compliance minimization to obtain truss-like structures to be used as preliminary STM layouts. Victoria, Querin and Mart [2] improved the proposed density approach by incorporating different mechanical properties for steel and concrete. Cai [3] proposed a density approach replacing the original tensile and compressive materials with isotropic materials with the same effective elasticity. Amir [4] presented a topology optimization procedure for reducing weight of concrete structures in which the distribution of both concrete and reinforcement bars is optimized simultaneously and concrete is modeled as a continuum exhibiting damage. Gaynor, Guest and Moen [6] proposed a hybrid method basically bringing together the density and the ground structure approaches for power path visualization in reinforced concrete structural elements. An orthotropic constitutive model in continuum elements represents the concrete material and discrete truss elements represent the steel reinforcement. Bilinear stress-strain relations were adopted to both concrete and steel. The optimization process involved simultaneously the discrete and the continuous elements, thus making the distinction of the compression and tension load paths. Bruggi [6] uses a density approach assuming concrete as a hyper-elastic material carrying only compression in which both the inherently nonlinear equilibrium equation and the energy-based topology optimization problem are solved within the same minimization procedure.

This paper presents an extension of the hybrid topology optimization approach [5] by applying the maximum filter [7] at the end of the optimization prosses to extract the final topology by means of eliminating fine bars. Tikhonov regularization is applied to the potential energy of the structure to solve singular equilibrium equations and check the equilibrium of the extracted solutions in the filtering procedure. Concrete is represented by plane elements associated with material density and steel is represented by bar elements associated with the cross-sectional area.

The remainder of this paper is organized as follows. Sections 2 and 3 present, respectively, the density methods and the ground structure approaches for topology optimization. Section 4 provides information on the topology optimization formulation of the hybrid method, along with some details of the implementation. In Section 5 some numerical examples and results are provided and the conclusions are presented in Section 6.

2 Density methods

Density methods for structural topology optimization operate in a region of the space where the structure is to be designed, called the extended domain (Ω), usually discretized in a finite element mesh for structural analysis. The optimization process consists of finding, in the extended domain under study, the distribution of material that minimizes the objective function, subject to volume constraint. The design variables are relative densities, ρe, given by the ratio of the volume of material to the volume of the element. Figure 1 illustrates the density method for the MBB beam presented in (a). Due to the symmetry of the problem, only half the beam is analyzed, thus delimiting the extended domain (b). Starting from a uniform density distribution, the redistribution of material occurs from one region to another, as shown in the intermediate solution (c), until the final topology (d) is obtained. Equation (1) presents the minimum compliance problem for the density approach using SIMP [8], [9], a penalization approach used to associate densities to material mechanical properties avoiding intermediate densities in the final solution.

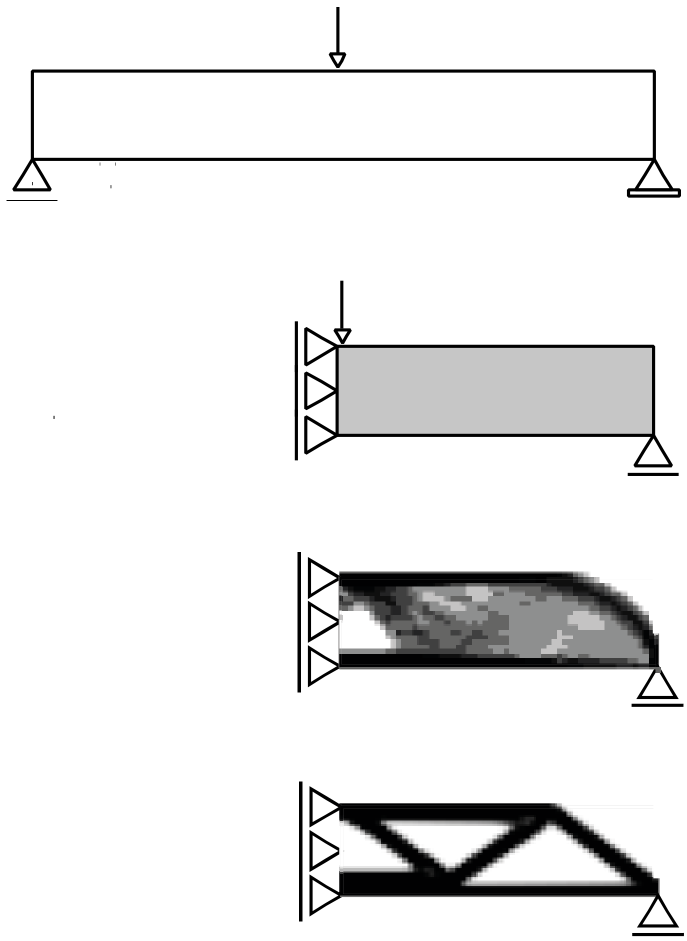

Figure 1 - Example of the topology optimization approach: (a) MBB beam; (b) extended domain; (c) intermediate solution; (d) final topology.

$$
\begin{array}{ll}
\text{Get:} & \boldsymbol{\rho} \\
\text{That minimizes:} & c(\boldsymbol{\rho}) = \mathbf{f}^{\mathrm{T}}\mathbf{u} \\
\text{Such that:} & \begin{cases} \dfrac{V(\boldsymbol{\rho})}{V_0} = f \\ 0 < \rho_{\min} \le \rho_{\mathrm{e}} \le 1 \end{cases} \\
\text{With:} & \begin{cases} \mathbf{K}\,\mathbf{u} = \mathbf{f} \\ E(\rho) = \rho^{p} E_0 \end{cases}
\end{array}
\qquad (1)
$$

Where: **u** represents the nodal displacement vector; **K** is the global stiffness matrix of the extended domain; **f** is the nodal force vector; **ρ** is the vector of the design variables; c is the objective function (minimum compliance of the structure); $V(\boldsymbol{\rho})$ represents the total material volume; V_0 represents the volume of the extended domain; f is the prescribed volume fraction; ρ_{min} is the minimum relative density; E_0 represents the Young's modulus of the solid material; and p is the penalty factor in SIMP.

The optimization problem in Eq. (1) is solved from the sensitivity analysis where the optimization algorithms lead to modifications in the design variables. The sensitivities of the compliance and the volume constraint are given, respectively, by Eq. (2) and Eq. (3). The sensitivity of the lateral constraints is -1, 0 or 1, depending on whether the constraint is related to the lower limit (-1 or 0) or to the upper limit (1 or 0).

$$\frac{\partial c}{\partial \rho_e} = -p\left(\rho_e\right)^{p-1} \mathbf{u}_\mathrm{e}^\mathrm{T}\, \mathbf{K}_0\, \mathbf{u}_\mathrm{e} \tag{2}$$

$$\frac{\partial R v_\rho}{\partial \rho_e} = V_e \tag{3}$$

3 The ground structure method

The ground structure method is a widely used numerical approach that removes unnecessary bars from a highly connected ground structure with fixed nodes and loads, resulting in an optimal topology with the corresponding cross-sections. Equation (4) presents the minimum compliance problem for the ground structure method.

$$\begin{aligned} &\text{Get:} && \mathbf{a} \\ &\text{That minimizes:} && c(\mathbf{a}) = \mathbf{f}^\mathrm{T}\, \mathbf{u}(\mathbf{a}) \\ &\text{Such that:} && \begin{cases} \mathbf{l}^\mathrm{T}\mathbf{a} - V^{max} \leq 0 \\ 0 < a_j^{min} \leq a_j \leq a_j^{max},\ j = 1,2,\dots,n \end{cases} \\ &\text{With:} && \mathbf{K}(\mathbf{a})\,\mathbf{u}(\mathbf{a}) = \mathbf{f} \end{aligned} \tag{4}$$

Where: **a** is a vector containing the design variables; c is the objective function (minimum compliance of the structure); **l** is a vector containing the length of the bars; V^{max} represents the maximum material volume; a_j^{min} and a_j^{max} are respectively the minimum and the maximum values for the cross-sectional area a_j.

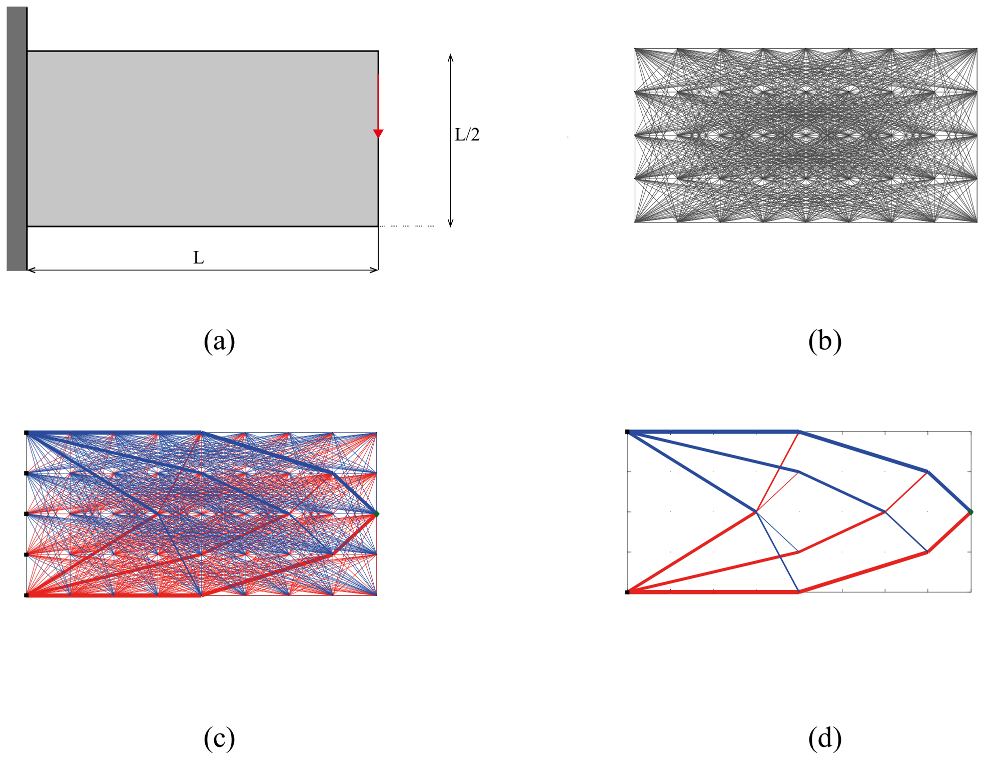

Figure 2 - Example of application of the ground structure method: (a) balance beam; (b) initial ground structure; (c) topology at the end of the optimization process, without cutting; (d) topology extracted after the cutting of bars.

Figure 2 illustrates the application of the ground structure method for compliance minimization of the cantilever beam (a). The ground structure is presented in (b) and the result of the optimization process in (c). The solution presented in (c) shows many thin bars that do little to contribute to the rigidity of the structure. Thus, in order to make the structure applicable in practical solutions, the bars with area below a cut-off parameter are eliminated at the end of the optimization, as shown in (d).

Ramos Jr. and Paulino [10] introduced the so-called discrete filter, represented mathematically by Eq. (5) for the extraction of the final topology, guaranteeing its equilibrium with the use of Tikhonov Regularization applied to the energy functional.

$$a_j = Filtro(\mathbf{a}, \alpha_f) = \begin{cases} 0 & se \ \dfrac{a_j}{\max(\mathbf{a})} < \alpha_f \\ a_j & \text{outro} \end{cases} \tag{5}$$

The optimization problem is then defined as:

$$\begin{array}{ll} \text{Get:} & \mathbf{a} \\ \text{That minimizes:} & c(\mathbf{a}) = \mathbf{f}^{\mathrm{T}}\ \mathbf{u}(\mathbf{a}) \\ \text{Such that:} & \begin{cases} \mathbf{l}^T\mathbf{a} - V^{max} \le 0 \\ 0 \le a_j \le a_j^{max} \end{cases} \\ \text{With:} & a_j = Filtro\ (\mathbf{a}, \alpha_f) \\ \text{e} & \min\limits_{\mathrm{u}} \Pi\ (\mathbf{u}(\mathbf{a})) + \dfrac{\lambda}{2}\mathbf{u}(\mathbf{a})^{\mathrm{T}}\ \mathbf{u}(\mathbf{a}) \end{array} \tag{6}$$

In order to apply this filter, it is necessary for the designer to provide the parameter α_f in Eq. (5), which can be an issue depending on the structure. Thus, Sanders, Ramos Jr. and Paulino [7] proposed the so-called maximum filter in order to obtain the largest possible value for the parameter α_f in each filter application so that the extracted topology satisfies the global equilibrium. This search is basically done by a bisection procedure in which the search bounds are null and unit values.

Similar to density methods, the sensitivity of the lateral constraints also assumes the value -1, 0 or 1. The sensitivities of the objective function and of the volume restriction according to Eq. (7) and (8), respectively.

$$\frac{\partial c}{\partial a_j} = -\mathbf{u}(\mathbf{a})^{\mathrm{T}}\ \mathbf{K}_{0b}\ \mathbf{u}(\mathbf{a}) \tag{7}$$

$$\frac{\partial Rv_{\mathrm{a}}}{\partial \mathrm{a}_{\mathrm{j}}} = l_j \tag{8}$$

4 Hybrid method

The density method (DM) and the ground structure method (GSM) are examples, respectively, of topology optimization with continuous and discrete representation of the design domain. One of the drawbacks of the GSM is that the solutions depend on the ground structure, and thus the possibilities of force flow are involuntarily limited by the designer when defining node and bars locations. The density method offers a free possibility of forming the force flow. However, it requires a post-processing to define the tension regions as discrete bars and thus produce representations that can be applied in practice. The principle of the hybrid approach is to combine a continuous representation with a discrete representation of the extended domain, the first one representing concrete and the second one to representing steel. The goal is to obtain consistent solutions to help designers to understand the flow of forces in reinforced concrete structures.

The extended domain is discretized with a hybrid mesh as shown in Fig. 3. A plane finite element mesh (Ωc) is used to represent the extended domain associated with the concrete material. A mesh of truss elements (Ωt) is used to represent the steel bars, connected to the first mesh. The plane finite element mesh is more refined because they represent small portions of the concrete extended domain. The mesh of truss elements is sparser and the transfer of forces occurs in the shared nodes. It is worth mentioning that the use of a denser ground structure generates more complex steel bar configurations in comparison to the solution obtained using a lower connectivity level.

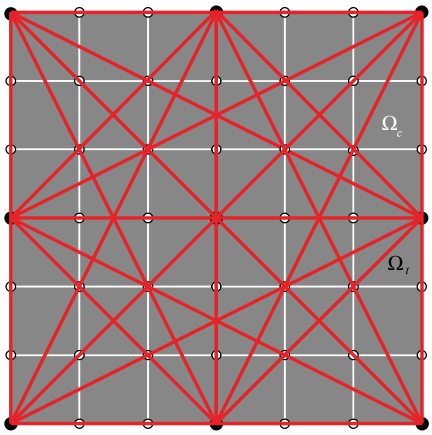

Figure 3 - Example of a hybrid mesh design domain

In this work the stress-strain diagrams of concrete and steel are represented by bilinear relations, as shown in Fig. 4. In order to force the tensile force lines to be represented preferably by the truss elements, a small value for the concrete Young's modulus in traction is adopted. In order to force the compression force lines to be exclusively represented by the plane elements, a null value is assumed for the steel Young's modulus in compression.

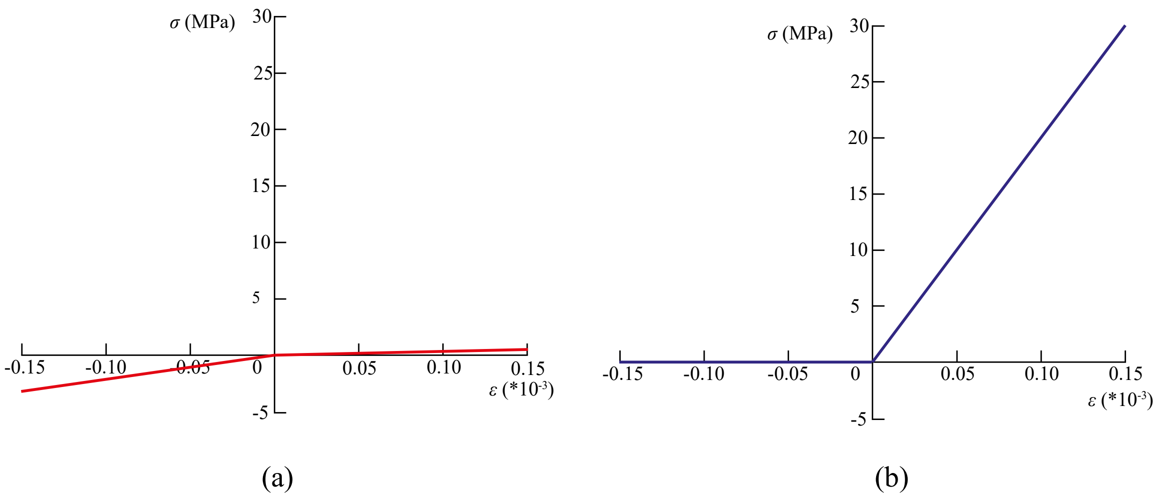

Figure 4 - Stress-strain relationship for: (a) concrete (b) steel.

The stiffness matrix of the hybrid topology is given by the assemblage of the stiffness matrices of the continuous and discrete elements, where the stiffness matrix of the discrete element ($\mathbf{K}_b$) is expressed according to Eq. (9) and the matrix of a continuous element ($\mathbf{K}_e$) described in Eq. (10).

$$\mathbf{K}_b = a_b \, \mathbf{K}_{0b} \tag{9}$$

$$\mathbf{K}_e = \rho_e^{\,p} \, \mathbf{K}_{0e} \tag{10}$$

Where: a_b represents the cross-sectional area of bar b; $\mathbf{K}_{0b}$ is the basic stiffness matrix of bar b in the global coordinate system; $\mathbf{K}_{0e}$ is the stiffness matrix of the continuous element e for solid material in the global coordinate system.

The topology optimization problem of the hybrid method to compliance minimization is presented in Eq. (11). The volume constraint is shared by the truss and the continuous topology.

$$\begin{aligned} &\text{Get:} && \mathbf{x} = [\mathbf{a}\,;\boldsymbol{\rho}] \\ &\text{That minimizes:} && c(\mathbf{a},\boldsymbol{\rho}) = \mathbf{f}^{\mathrm{T}}\mathbf{u} \\ &\text{Such that:} && \begin{cases} \sum_{b\in\Omega_t} l_b^{\mathrm{T}} a_b + \sum_{e\in\Omega_c} \rho_e V_e \le V^{max} \\ 0 \le a_b \quad \forall\, b\in\Omega_t \\ 0 \le \rho_e \le 1 \quad \forall\, e\in\Omega_c \end{cases} \\ &\text{With:} && \begin{cases} \mathbf{K}(\mathbf{a},\boldsymbol{\rho})\,\mathbf{u} = \mathbf{f} \\ E_b\,(a) \\ E_e\,(\rho) = \rho_e^{\,p}\, E_{0e} \end{cases} \end{aligned} \tag{11}$$

To evaluate the Young's modulus to be associated with the continuous elements depends on the maximum principal normal stress, whether tensile or compressive, according to Fig. 4. The principal normal tensile and compressive stresses are evaluated according to Eq. (12). For the discrete elements, the tension in the bar is evaluated by Eq. (13).

$$\sigma_{\substack{\max\\ \min}} = \frac{\sigma_x + \sigma_y}{2} \pm \sqrt{\left(\frac{\sigma_x - \sigma_y}{2}\right)^2 + \tau_{xy}^{\;2}} \tag{12}$$

$$\sigma_{xm} = \frac{f_b}{a_b} \tag{13}$$

Where: σ_x represents the normal stress with respect to the x axis; σ_y represents the normal stress with respect to the y axis; τ_{xy} represents the shear stress normal to the plane of the x axis according to the direction of the y axis; σ_{max} is the maximum principal normal stress; σ_{min} is the minimum principal normal stress; σ_{xm} is the normal stress with respect to the x-axis; f_b is the normal force on the bar; a_b is the cross sectional area of the bar.

In the implementation carried out in this paper a normalization of the design variables associated to the area of the bars is adopted, according to Eq. (14), in order to have the same magnitude for both densities and areas.

$$\rho_a = \frac{\mathbf{a}}{a_{max}} \tag{14}$$

Where ρ_a is the density and a_{max} is the prescribed maximum area in the ground structure method.

The sensitivities of the objective function and volume constraint with respect to the densities (Eq.(2) and (3)) remain unchanged while the sensitivities with respect to the areas (Eq.(7) and (8)) become, respectively:

$$\frac{\partial c}{\partial \rho a_j} = -\mathbf{u}(\boldsymbol{\rho}\mathbf{a})^{\mathrm{T}}\,\mathbf{K_0}\,\mathbf{u}(\boldsymbol{\rho}\mathbf{a})\,a_{max} \tag{15}$$

$$\frac{\partial Rv_{\rho a}}{\partial \rho a_j} = \mathbf{l}^{\mathrm{T}}\,a_{max} \tag{16}$$

5 Results

This section presents results of the implementation of the hybrid method: a MBB beam; a deep beam with a cutout; and a hammerhead bridge pier. All problems are solved using Q4 plane finite elements in the continuous mesh. The penalty factor of the SIMP model is equal to 3, r_{min} in the sensitivity filter to avoid numerical instabilities is 1.5 times the length of the square element of the continuous mesh. The Poisson ratio ν is 0.20 and the Young's modules for steel are 200 GPa in traction and zero in compression, while the modules for concrete are 24.9 GPa in compression and 2.0 GPa in traction. Convergence of the optimization process is achieved when the relative change in the norm of the design variables in consecutive iterations is less than 1%.

5.1 The MBB beam

The first example is the MBB beam presented in Fig. 5(a) with L = 5 m. The problem was solved for a continuous mesh with 3600 square elements with dimension 0,0416 m and a truss mesh with 270 bar elements presented in Fig. 5(b). The prescribed volume fraction is 55% of the volume of the design domain.

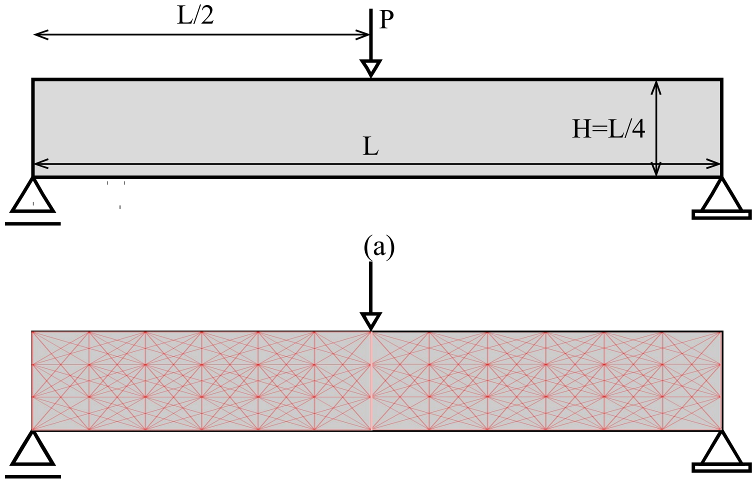

(a)

(b)

Figure 5 - MBB beam: (a) design domain; (b) mesh.

Figure 6 present the solution for the example presented in Fig. 5 using the hybrid topology optimization procedure. As previously discussed, the compressive load paths are idealizations of the stress fields in the concrete and may assume any form. Tension load paths, on the other hand, assume rectilinear shapes, and therefore represent the rebar more precisely.

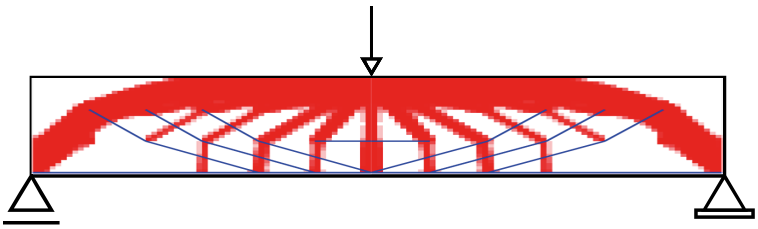

Figure 6 - Optimized topologies for the MBB beam.

5.2 The hammerhead bridge pier

The second example is the hammerhead bridge pier presented in Fig. 7(a) with L = 12 m. The problem was solved for a continuous mesh with 7708 square elements with dimension 0,1666 m on the x axis and a truss mesh with 1588 bar elements presented in Fig. 7(b). The prescribed volume fraction is 50%

of the volume of the design domain.

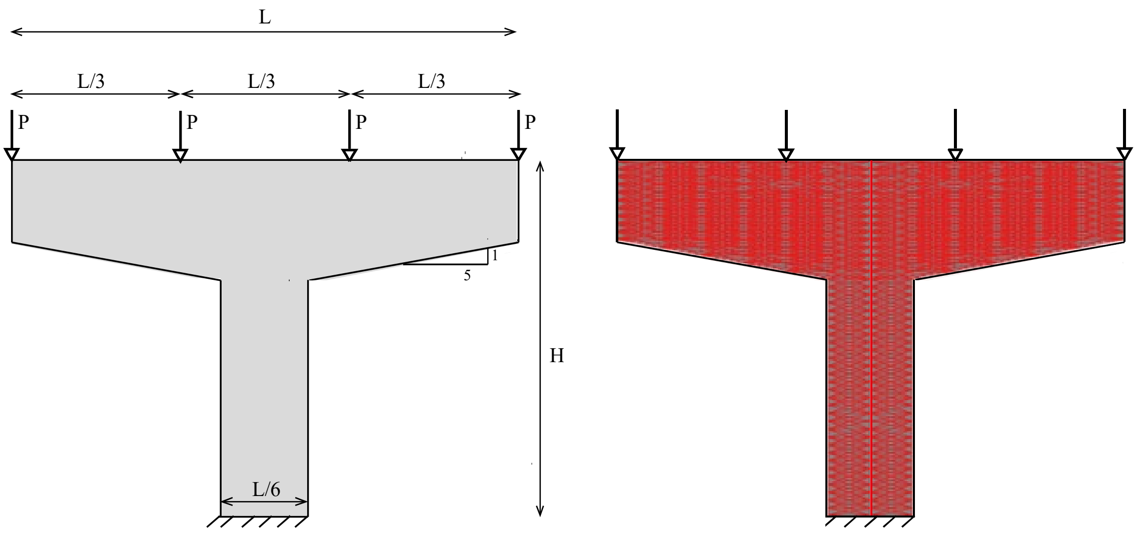

Figure 7 - The hammerhead bridge pier: (a) design domain; (b) mesh.

Figure 8 present the solution for the example presented in Fig. 7. The solution is consistent with the models used in practice for this kind of structure.

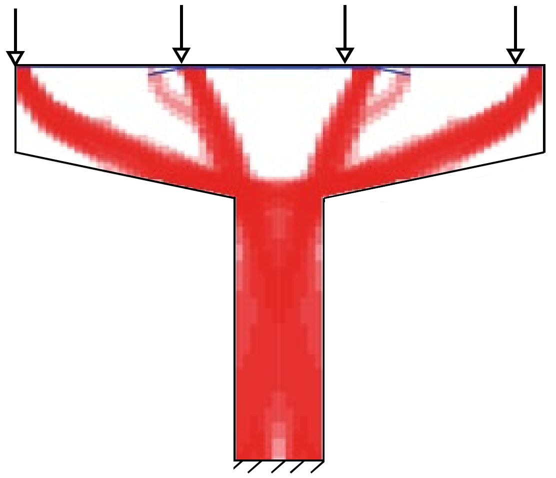

Figure 8 - Optimized topology for the hammerhead píer.

5.3 The deep beam with hole and a cutout

The third example is the deep beam with a hole and a cutout presented in Fig. 9(g) for with $L = 5$ m. In order to analyze the role played by the hole and by the cutout int the load paths a beam none of these elements was analyzed (Fig. 9(a)) and in the sequence each of these elements was added as shown in Fig. 9(c) and Fig. 9(e), all with square elements with dimension 0,0416 m. The problem presented in Fig. 9(a) was solved for a continuous mesh with 7200 elements and a truss mesh with 1570 bar elements presented in Fig. 9(b). The problem presented in Fig. 9(c) was solved for a continuous mesh with 6192 elements and a truss mesh with 1335 bar elements presented in Fig. 9(d). The problem presented in Fig. 9(e) was solved for a continuous mesh with 6300 elements and a truss mesh with 1370 bar elements presented in Fig. 9(f). The problem presented in Fig. 9(g) was solved for a continuous mesh with 5292 elements and a truss mesh with 1135 bar elements presented in Fig. 9(h). In all cases the prescribed volume fraction is 35% of the volume of the design domain.

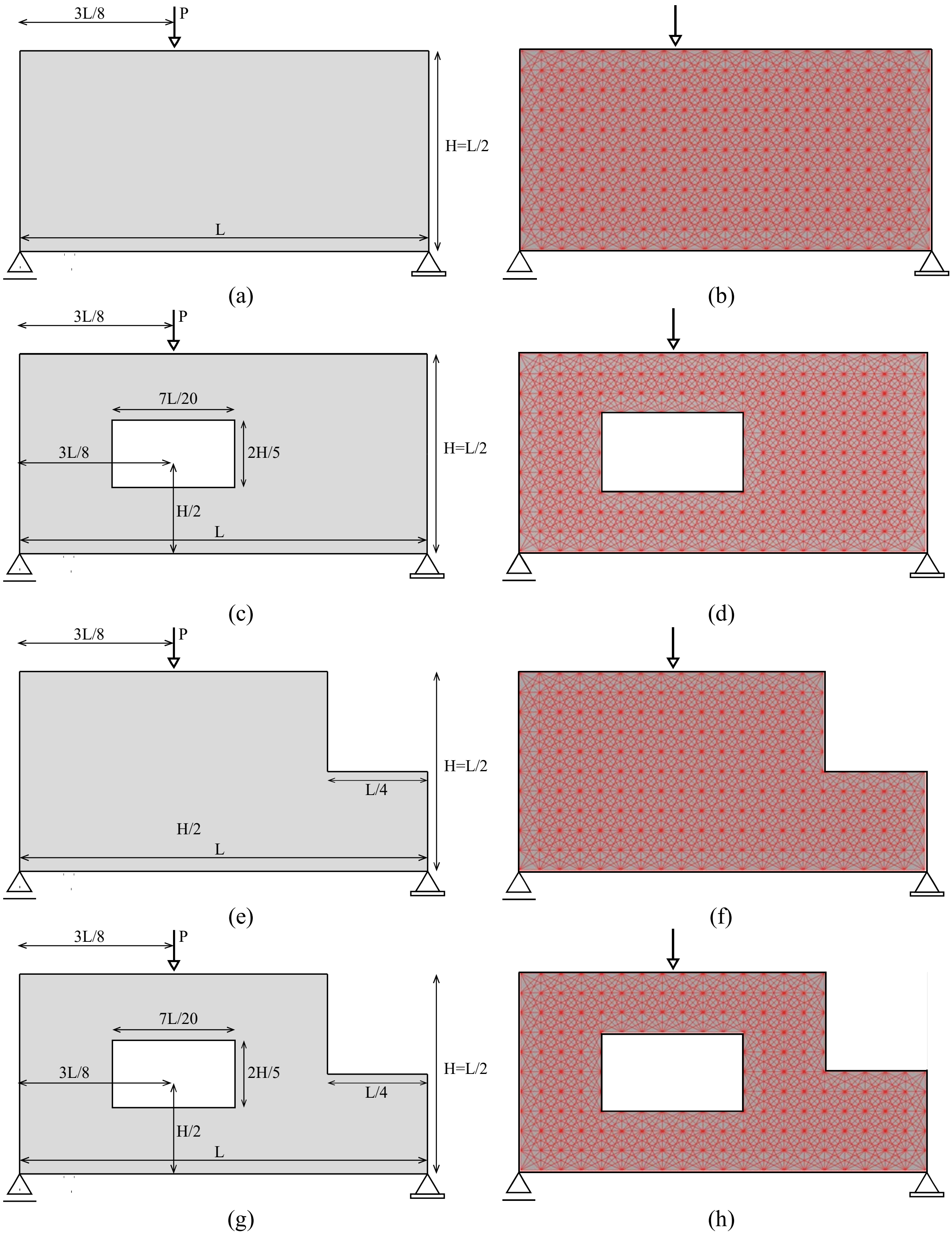

Figure 9 - Deep beam: (a) design domain for the massive beam; (b) mesh for the massive beam; (c) design domain for the beam with a hole; (d) mesh for the with a hole; (e) design domain for the beam with cutout; (f) mesh for the with a cutout; (g) design domain for the beam with a hole and a cutout; (h) mesh for the with a hole and a cutout.

The solutions for the deep beams in Fig. 9 are presented in Fig 10. Figures 10(a) and 10(b) demonstrate that the presence of the hole divert the compressive flow and enhance its thickness in the region bellow the load point. As a consequence, tensile bars are added at that region. Figure 10(c) shows that the cutout deviate the compressive flow in that region, changing the position of the tensile bars.

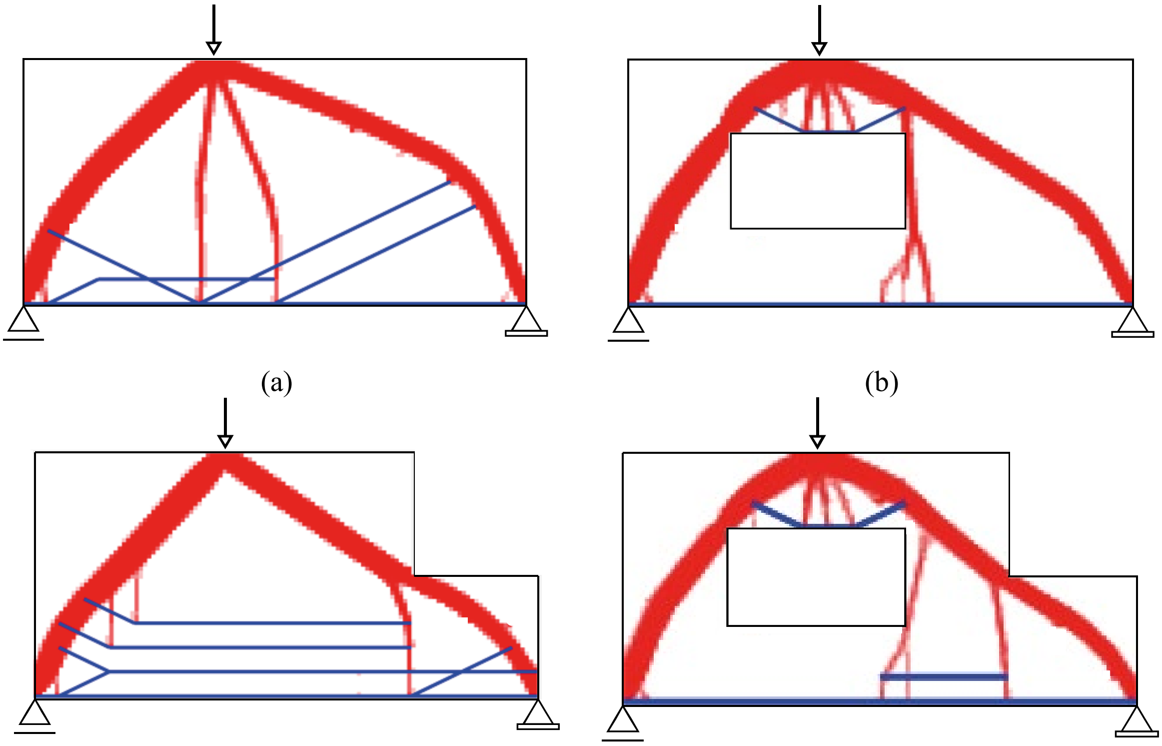

(a) (b) (c) (d)

Figure 10 - Optimized topologies using the hybrid optimization algorithm: (a) massive deep beam; (b) deep beam with hole; (c) deep beam with a cutout; (d) deep beam with a hole and a cutout.

6 Conclusions

The solutions obtained for the MBB beam and the hammerhead bridge pier resemble a blend of the solutions of these structures separately optimized by the density method and the structure ground structure method, exposed in the work by Gaynor, Guest and Moen [5]. The solution for the deep beam with a hole and a cutout resembles the continuous solution also presented in [5] due to the appearance of risers close to the necessary supports due to traction developed by force scattering at these locations. The results show that topology optimization can provide effective solutions to design RC structures and that the orthotropic model used in [5] has little influence on the final topology compared to the result obtained with the isotropic model used in this work.

The main contribution of this work is to provide a numerical tool to help designers to understand the flow of forces in complex reinforced concrete structures. This work offers room for extensions such as the extension of the concepts of the maximum filter for the plane state elements associated to the material densities. In addition, the present work can be naturally extended to three-dimensional problems.

Acknowledgments

The authors thank the support of FAPEG and CNPq for the financial support provided by project

07/2016.

References

[1] M. Bruggi. Generating strut-and-tie patterns for reinforced concrete structures using topology optimization. *Computer & Structures*, vol. 87, n. 23-24, pp. 1483–1495, 2009.
[2] M. Victoria; O. M. Querin; P. Marti. Generation of strut-and-tie models by topology design using different material properties in tension and compression. *Structure and Multidisciplinary Optimization,* vol 44, pp. 247–258, 2011.
[3] K. Cai. A simple approach to find optimal topology of a continuum with tension-only or compression-only material. *Structural and Multidisciplinary Optimization*, v.43, p. 827-835, 2011.
[4] O. Amir. A topology optimization procedure for reinforced concrete structures. *Computers & Structures,* v. 114–115, pp 46–58, 2013.
[5] A.T.Gaynor; J.K.Guest; C.D.Moen. Reinforced concrete force visualization and design using bilinear truss-continuum topology optimization. *ASCE Journal of Structural Engineering*, vol. 139, n. 4, pp. 607-618, 2013.
[6] M. Bruggi, A numerical method to generate optimal load paths in plain and reinforced concrete structures. *Computers & Structures*, v. 170, pp. 26–36, 2016.
[7] E. D. Sanders; A. S. Ramos Jr; G. H. Paulino. A maximum filter for the ground structure method: An optimization tool to harness multiple structural designs. *Engineering Structures*, v. 151, n. 1, p. 235-252, 2017.
[8] M. P. Bendsøe. Optimal shape design as a material distribution problem. *Structural Optimization*, v. 1, n. 4, pp. 193-202, 1989
[9] M.Zhou; G. I. N.Rozvany The COC Algorithm .2. Topological, Geometrical and Generalized Shape Optimization. *Computer Methods in Applied Mechanics and Engineering*, v. 89, n. 1-3, pp. 309-336.
[10] A. S. Ramos Jr; G. H. Paulino. Filtering structures out of ground structures - a discrete filtering tool for structural design optimization. *Structural and Multidisciplinary Optimization*, v. 54, n. 1, pp. 95-116, 2016.